View Article Online / Journal Homepage / Table of Contents for this issue

Multiple mode coupling in Cy3 molecules by impulsive coherent vibrational spectroscopy using a few-cycle laser pulse†

Takahiro Teramoto*[ab] and Takayoshi Kobayashi[abcd]

Received 14th May 2010, Accepted 24th August 2010
DOI: 10.1039/c0cp00567c

Published on 20 September 2010. Downloaded by National Chiao Tung University on 25/04/2014 07:35:27.

Multiple vibrational mode coupling that induces the missing mode effect and Duschinsky rotation on the potential energy surface of the S_1 state in the Cy3 molecule was clarified by real-time ultrafast spectroscopy with a few-cycle laser pulse. The contributions of homogeneous and inhomogeneous dephasing to the total dephasing time were found to be 55% and 45%, respectively.

As a result of recent progress in microscopy, dye molecules are frequently used to label the functions of cultured cells *in vivo* and *in vitro* because a high spatial resolution that exceeds the diffraction limit (*i.e.*, under 100 nm) can be achieved using fluorescence from dye molecules.[1–4] In these applications, photochromic molecules or optical switching using the Förster resonance energy transfer (FRET) mechanism are frequently used. Cyanine Cy3 molecules are famous for their high fluorescence efficiency and highly efficient FRET activity when combined with the Cy5 molecule.[4] Despite being extensively used in biological applications, there have been surprisingly few spectroscopic investigations of the Cy3 molecules.[5,6] Especially, there is no report about the ultrafast dynamics on the potential energy surface in the excited state.

Linear spectroscopy techniques that employ stationary absorption and spontaneous fluorescence are conventional techniques that provide information on homogeneous and inhomogeneous broadening. However, nonlinear spectroscopic techniques, such as photon echo spectroscopy, must be used to investigate homogeneous dephasing dynamics.[7] In a previous paper, we demonstrated that the electronic dephasing time and the excited-state vibrational dynamics can be obtained from real-time traces in a "negative-time" range in a pump–probe experiment using a pulse that is much shorter than the electronic dephasing time and the excited-state molecular vibration period.[8] This technique has the advantage that it simultaneously obtains information about the electronic and vibrational dephasing dynamics from a single experimental data set.

[a] *Department of Applied Physics and Chemistry and Institute for Laser Science, University of Electro-Communications, 1-5-1 Chofugaoka, Chofu, Tokyo, 182-8585, Japan. E-mail: teramoto@ils.uec.ac.jp; Fax: +81-42-443-5826; Tel: +81-42-443-5846*
[b] *International Cooperative Research Project (ICORP), Japan Science and Technology Agency, 4-1-8 Honcho, Kawaguchi, Saitama 332-0012, Japan*
[c] *Department of Electrophysics, National Chiao Tung University, Hsinchu 30010, Taiwan*
[d] *Institute of Laser Engineering, Osaka University, 2-6 Yamada-oka, Suita, Osaka565-0871, Japan*

† Electronic supplementary information (ESI) available: Experimental details and phase relaxation dynamics are supplied. See DOI: 10.1039/c0cp00567c

In this communication, we demonstrate how to extract molecular vibrational modes that are coupled with each other but buried by combining both linear and nonlinear spectroscopic data according to the idea of both Duschinsky rotation[9,10] and missing mode effect[11,12] for the first time. This technique reveals multiple-mode coupling on the potential surface of the excited state of Cy3 molecules. Additionally, from the absorbance change data in the "negative time" range we determine the relative contributions of homogeneous and inhomogeneous dephasing to the total dephasing time.

The Cy3 sample was purchased from GE Healthcare Bio-Sciences KK. The molecular structure of Cy3 molecule studied in this communication is depicted in Scheme 1. Cy3 was dissolved in pure water. Stationary absorption and fluorescence spectra were recorded with an absorption spectrometer (Shimadzu, UV-3101PC) and a fluorophotometer (Hitachi, F-4500), respectively. Resonance Raman spectra were measured using the 488 nm line from an Ar^+-ion laser. The ultrafast spectroscopy procedure has been described in ESI† in detail, and a brief description is given here. Both pump and probe pulses were generated by using a noncollinear optical parametric amplifier (NOPA) system developed in our group.[13] The pump source of this system is a commercially available regenerative amplifier (Spectra-Physics, Spitfire) that has a pulse duration of 50 fs, a center wavelength of 790 nm, a pulse repetition rate of 5 kHz, and an average output power of 800 mW. The visible NOPA pulse with a duration of 6.2 fs covered the photon energy range 1.69–2.37 eV, with a constant spectral phase over the whole laser spectrum. Pump–probe signals were detected with a 128-channel lock-in amplifier. Real-time vibrational spectra were measured for delay times between the pump (40 nJ) and probe pulses (2 nJ) in the range −100 to 1100 fs in 1 fs intervals.

Fig. 1(A) shows the stationary absorption and fluorescence spectra of Cy3. Their spectra exhibit quasi-mirror symmetry with respect to the mirror plane at 2.21 eV with the Stokes shift of 0.1 eV. One shoulder in both the absorption and fluorescence spectra reveals vibrational progression. The vibrational progression from the band origin (2.26 eV) is 144 meV (1160 cm^{-1}) in the absorption spectrum, whereas the energy separation from the band origin (2.16 eV) is 100 meV

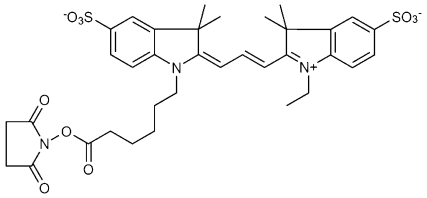

Scheme 1 Molecular structure of Cy3 molecule.

View Article Online

Published on 20 September 2010. Downloaded by National Chiao Tung University on 25/04/2014 07:35:27.

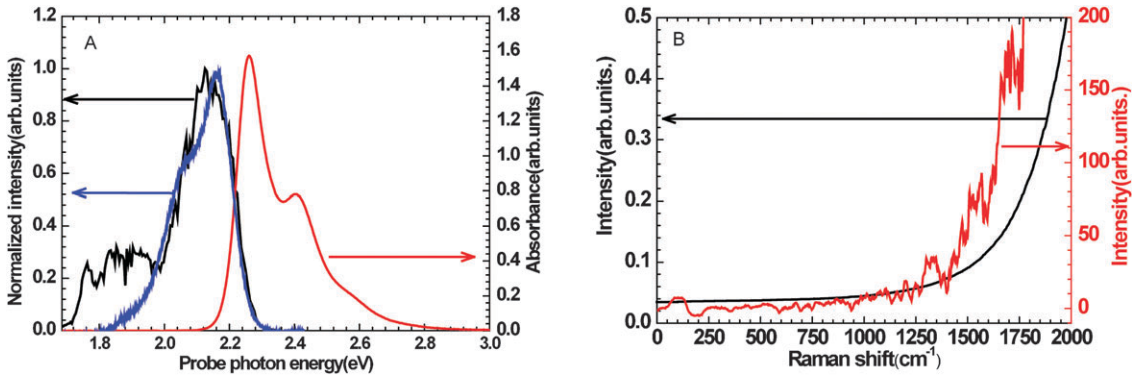

Fig. 1 (A) Stationary absorption spectrum and fluorescence spectrum of Cy3 molecules and laser spectrum. (B) Resonance Raman spectrum excited at 488 nm. Second derivative of the Raman data with respect to wave number .

(807 cm^{-1}) in the fluorescence spectrum. The uncertainty of the vibrational progression inherent due to the overlap of multiple peaks exists. Based on the results of several studies of cyanine molecules,[14–16] they can be assigned as collective symmetric modes, which mainly involve motions of the bridging C atoms between two aromatic rings in the Cy3 molecule.

Fig. 1(B) shows a resonant Raman spectrum of the Cy3 dye excited at 488 nm. Because of intense spontaneous fluorescence and the weak signal due probably to small Raman cross sections of the molecular vibrational modes, the S/N of Raman spectrum is small. To determine the frequencies of Raman peaks, the second derivative of the Raman signal with respect to wave number was used (red curve in Fig. 1(B)). However, no clear molecular vibration signature could be identified. We interpret these results as follows. The contribution of molecular vibrational modes to the stationary absorption spectrum depends on the vibronic coupling strength of each mode. In the case of Cy3, the 1160 cm^{-1} mode has the highest vibronic coupling strength of all the modes in the stationary absorption spectrum. The differences between the absorption and fluorescence spectra of this vibrational mode can be explained by Duschinsky rotation on the S_1 excited-state potential hypersurface with geometrical relaxation after photoexcitation.[9,10]

Fig. 2(A) shows a two-dimensional plot of the absorbance change (ΔA) of the Cy3 dye for pump–probe delay times in the range −100 to 1100 fs over the whole probe spectral range. Coherent artifacts are visible in the ΔA spectra in the range 0 to 100 fs. As seen in Fig. 2(B) and (C), both the signal intensity and the spectral profile remain constant in the range 100 to 1100 fs because of the much longer lifetime of the S_1 state. As discussed in previous papers by our group,[8] when the probe pulse precedes the pump pulse, the probe delay time dependence of the signal reveals information about the electronic polarization induced by the probe pulse. (In the present paper, this time range is referred to as the "negative-time" range.) In this range, the probe pulse generates electronic coherence in the sample within electronic dephasing time. Then, the intense pump field forms a grating which interacts with another pump-field to be diffracted into the probe direction, satisfying the causality. The phase relaxation time of the relevant electronic states can be obtained from the

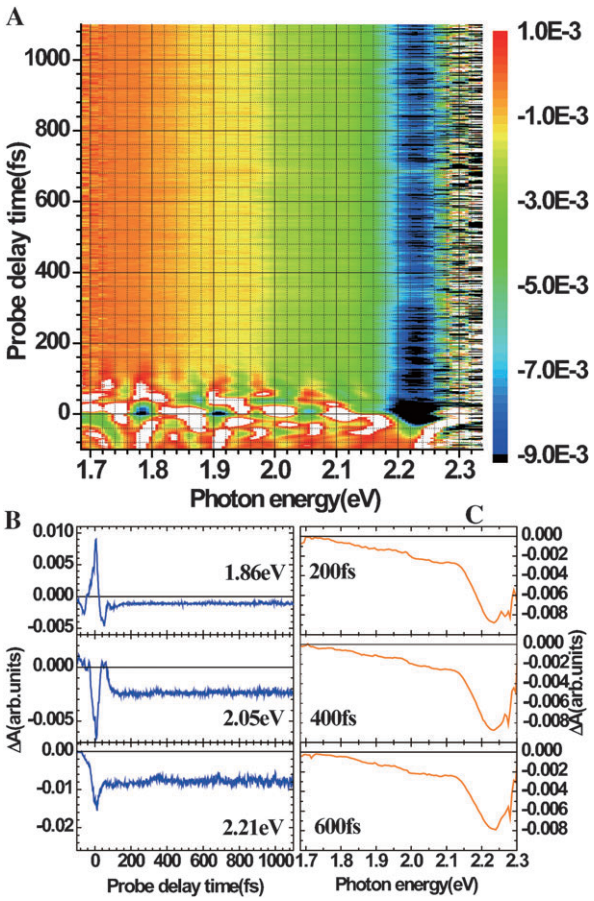

Fig. 2 Two-dimensional real-time absorbance difference spectrum of Cy3. (A) Two-dimensional plot of $\Delta A(\omega, t)$ of Cy3. (B) Real-time traces of ΔA at photon energies of 1.86, 2.05, and 2.21 eV. (C) Photon energy dependencies of ΔA at delay times of 200, 400, and 600 fs.

ΔA data with the delay time dependence in the negative-time region.

The dephasing rate ($1/T_2^{ele}$) obtained from the plot consists of the following three components:

$$\frac{1}{T_2^{ele}} = \frac{1}{2T_1^{ele}} + \frac{1}{T_2'^{ele}} + \frac{1}{T_2^{*ele}}. \quad (1)$$

 This journal is © the Owner Societies 2010

View Article Online

Published on 20 September 2010. Downloaded by National Chiao Tung University on 25/04/2014 07:35:27.

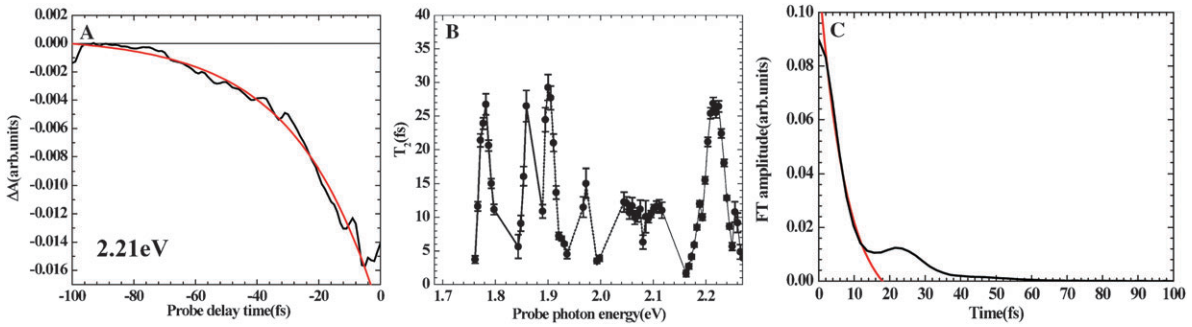

Fig. 3 (A) $\Delta A(t)$ in the negative-time region of Cy3 at 2.21 eV and fitting result. (B) The probe photon energy dependence of the electronic dephasing time of Cy3. Solid lines connect adjacent channels of 128-ch lock-in amplifier, while dashed lines connect non-adjacent channels. (C) Inverse Fourier transform spectra of the stationary absorption spectra of Cy3 and fitting result (see ESI†).

Here, T_1^{ele} is the population decay time, and $T_2'^{ele}$ and T_2^{*ele} are, respectively, the pure electronic dephasing time and the electronic phase relaxation time due to inhomogeneous broadening. For simplicity, we assume that $T_2'^{ele} = \infty$. By analyzing the plot in Fig. 3, the electronic dephasing time was found to be $T_2^{ele} = 27 \pm 1$ fs. From the population decay time $T_1^{ele} > 1$ ps in the previous section, $1/T_1^{ele}$ can be approximated as 0. As a result, the *pure* electronic dephasing time is determined to be $T_2'^{ele} = 27 \pm 1$ fs. The negative time data correspond to the dynamic response of the macroscopic polarization induced by the resonant overlap of the laser spectrum and the absorption spectrum of Cy3 molecule. This overlap is limited mainly in the region of the lowest absorption peak. Consequently, the effect of inhomogeneity is limited and it is mainly caused by electronic inhomogeneity rather than vibrational inhomogeneity. Therefore, we assume that the inhomogeneity in the overlapping range is negligibly small. Based on these considerations, the pure electronic dephasing time found is considered to be accurate.

To determine the fractional contributions of homogeneous and inhomogeneous dephasing to the total dephasing, we took the Fourier transform of the stationary absorption spectra. The resultant data indicate a damped oscillator with a total dephasing time of 15 ± 2 fs (Fig. 3(C)). From this electronic dephasing time, we found that homogeneous and inhomogeneous dephasing, respectively, contribute 55% and 45% to the total dephasing time.

The probe delay time (t) dependent change ($\delta\Delta A(\omega, t)$) in $\Delta A(\omega, t)$ is due to the molecular vibration. Fig. 4 shows a two-dimensional (ω, t) plot of the fast Fourier transform (FFT) power spectra of real-time traces of ΔA (ω, t) probed at the 128 photon energies shown in Fig. 2. Molecular vibrational modes are expected to be observed because the pulse duration of the pump laser is much shorter than the molecular vibration period and the ΔA signal is generated by a $\chi^{(3)}$ process, which obeys the same selection rule in the Raman spectrum. Fig. 4(B) shows the integrated FFT power spectrum of Cy3 in the region 1.85 to 2.2 eV. The peak corresponding to the 1160 cm^{-1} mode appears at 1139 cm^{-1}. The uncertainty in the FFT spectra is about 30 cm^{-1}. However, it is difficult to assign the 807 cm^{-1} mode in the FFT spectra. The other peaks can be assigned to molecular vibrations.

We consider why absorption and fluorescence spectra exhibit only a single vibrational progression despite the fact that the molecular vibration signals appear in FFT power spectra obtained by real-time spectroscopy. To determine the cause for this, we invoked the missing mode effect (MIME)[11,12] when analyzing vibrational modes in the real-time spectra. In the MIME model, fluorescence spectra can be modeled by a damped harmonic oscillator. The correlation function that describes the wave packet motion on the

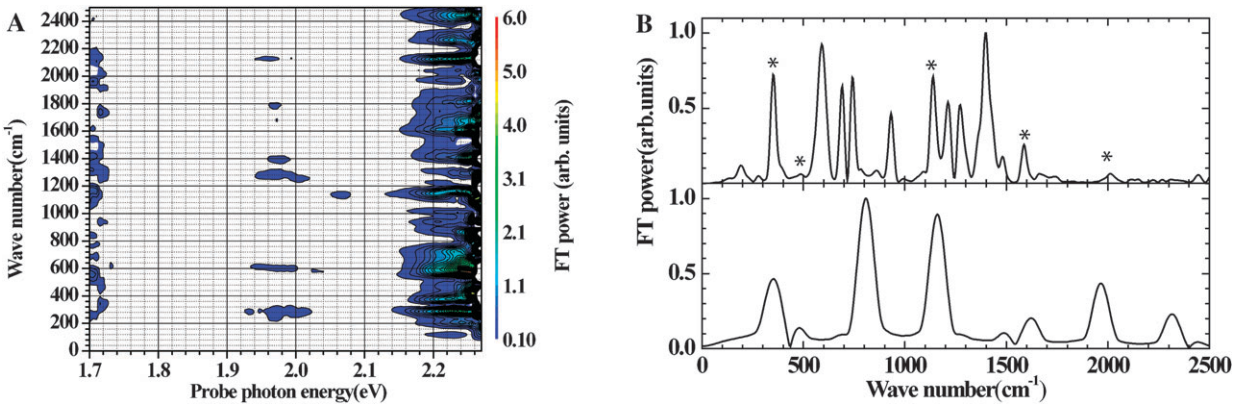

Fig. 4 Two-dimensional plot of FFT power spectra of Cy3 (A). Two-dimensional plot of FFT power spectra of Cy3 (B). (Top) Integrated FFT power spectra of Cy3 in the region 1.85 to 2.2 eV. (Bottom) FFT power spectra extracted from the MIME model.

View Article Online

Published on 20 September 2010. Downloaded by National Chiao Tung University on 25/04/2014 07:35:27.

potential energy surface in the excited state can be formulated as follows:

$$\langle\phi_0|\phi(t)\rangle = \prod_k(\langle\phi_{0k}|\phi_k(t)\rangle)\exp(-iE_0t/\hbar - \Gamma^2t^2)$$

$$(\langle\phi_{0k}|\phi_k(t)\rangle) = \exp(-(\Delta_k^2/2)(1 - e^{-i\omega_kt}) + i\omega_kt/2) \quad (2)$$

Here, ϕ_{0k} and $\phi_k(t)$ represent the wave packets with energy difference E_0 and displacement Δ_k of the minimum position of the potential energy surface between the ground and excited states of the kth mode. The correlation function between ϕ_0 and $\phi(t)$ represents a damped oscillator that consists of several damped oscillators with a frequency ω_k.

Because the 807 cm^{-1} mode appears in the fluorescence spectrum, we treated this mode as a damped oscillator with the above-derived total dephasing time of 15 fs. Because this damped oscillator is due to the interference between molecular vibrational modes, we can extract contributed molecular vibrational modes if we can get the information of mode coupling. From the discussion about stationary absorption and fluorescence spectra, the 1160 cm^{-1} mode is assumed to couple most strongly with the 807 cm^{-1} mode according to the Duschinsky rotation. To extract other coupling modes, Fourier transforms were taken of the spectrum of the damped oscillator with 807 cm^{-1} divided by that of the damped oscillator with 1160 cm^{-1}. The resultant spectrum is shown at the bottom of Fig. 4(B). By comparing with the experimental results, we find that the modes at 350, 480, 1139, 1480, 1600, and 2000 cm^{-1} couple with each other and produce the 807 cm^{-1} mode in the fluorescence spectra. This result demonstrates that multiple vibrational mode coupling occurs on the potential energy surface of the S_1 state of Cy3.

In summary, the electronic dephasing time of Cy3 is determined to be 27 ± 1 fs from real-time absorbance difference spectra in the time range in which the probe pulse proceeds the pump pulse. The electronic phase-relaxation dynamics was obtained by taking the Fourier transform of the stationary absorption spectra. The contributions of homogeneous and inhomogeneous dephasing to the total dephasing time were found to be 55% and 45%, respectively. Additionally, we found that Cy3 molecules exhibit very weak molecular vibrational coherence in real-time ultrafast spectroscopy although vibrational modes appear in both stationary absorption and fluorescence spectra. By applying MIME analysis, we have found the multiple mode coupling dynamics on the potential surface of the S_1 state in Cy3 molecules. These analytical techniques, which permit the determination of the dephasing time and the ratio of the homogeneous and inhomogeneous dephasing times and the extraction of multi-mode coupling based on the MIME model, are powerful tools for investigating the molecular dynamics in condensed phases.

Acknowledgements

The authors thank Prof. Tokunaga and his students for their help in the Raman measurement. This work was partly supported by a grant from the Ministry of Education (MOE) in Taiwan under the ATU Program at National Chiao Tung University. A part of this work was performed under the joint research project of the Institute of Laser Engineering, Osaka University under Contract No. B1-27. T. Teramoto was supported by a Grant-in-Aid for Young Scientists (B) (2174022) from the Japan Society for the Promotion of Science.

References

1 M. Bates, B. Huang, G. T. Dempsey and X. Zhuang, *Science*, 2007, **317**, 1749.
2 H. Neuweiler and M. Sauer, *Anal. Chem.*, 2005, **77**, 178A.
3 Y. C. Cao, R. Jin, J. Nam, C. S. Thaxton and C. A. Mirkin, *J. Am. Chem. Soc.*, 2005, **125**, 14676.
4 M. Bates, T. R. Blosser and X. Zhuang, *Phys. Rev. Lett.*, 2005, **94**, 108101.
5 K. Jia, Y. Wan, A. Xa, S. Li, F. Gong and G. Yang, *J. Phys. Chem. A*, 2007, **111**, 1593.
6 F. Köhn, J. Hofkens, R. Gronheid, M. V. D. Auweraer and F. C. D. Schryver, *J. Phys. Chem. A*, 2002, **106**, 4808.
7 S. Mukamel, *Principles of Nonlinear Optical Spectroscopy*, Oxford University Press, 1995.
8 T. Kobayashi, J. Du, W. Feng and K. Yoshino, *Phys. Rev. Lett.*, 2008, **101**, 037402.
9 F. Duschinsky, *Acta Physicochim. URSS*, 1937, **7**, 551.
10 T. Fuji, T. Saito and T. Kobayashi, *Chem. Phys. Lett.*, 2000, **332**, 324.
11 L. Tutt, D. Tannor, J. Schindler, E. J. Heller and J. I. Zink, *J. Phys. Chem.*, 1983, **87**, 3017.
12 L. Tutt and J. I. Zink, *J. Am. Chem. Soc.*, 1986, **108**, 5830.
13 T. Kobayashi, Z. Wang and I. Iwakura, *New J. Phys.*, 2008, **10**, 065009.
14 H. Mustroph, K. Reiner, J. Mistol, S. Ernst, D. Keil and L. Hennig, *ChemPhysChem*, 2009, **10**, 835.
15 T.-S. Yang, M. S. Chang, R. Chang, M. Hayashi, S. H. Lin, P. Vöhringer, W. Dietz and N. F. Scherer, *J. Chem. Phys.*, 1999, **110**, 12070.
16 T. Kobayashi, Y. Wang, Z. Wang and I. Iwakura, *Chem. Phys. Lett.*, 2008, **466**, 50.

 This journal is © the Owner Societies 2010